Journal of Molecular Structure 1054–1055 (2013) 164–169

Contents lists available at ScienceDirect

Journal of Molecular Structure

journal homepage: www.elsevier.com/locate/molstruc

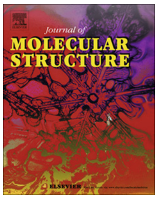

Synthesis, electrochemistry and liquid crystal properties of 1,2,3-(NH)-triazolylferrocene derivatives

Hai-Ying Zhao, Le Guo, Shu-Feng Chen, Zhan-Xi Bian *

College of Chemistry and Chemical Engineering, Inner Mongolia University, Huhhot 010021, China

HIGHLIGHTS

- The ferrocene derivatives containing 1,2,3-triazole ring were prepared.
- These compounds exhibit good absorption, emission and electrochemical properties.
- The liquid crystal properties of this kind of compound were firstly investigated.

ARTICLE INFO

Article history:
Received 28 August 2013
Received in revised form 20 September 2013
Accepted 23 September 2013
Available online 1 October 2013

Keywords:
Ferrocene
1,2,3-Triazole
Electrochemistry
Liquid crystal

ABSTRACT

A series of aryl(5-ferrocenyl-2*H*-1,2,3-triazol-4-yl)methanone **3a–3d** have been firstly synthesized and characterized. The X-ray crystal structure of phenyl(5-ferrocenyl-2*H*-1,2,3-triazol-4-yl)methanone **3a** confirms that 1,2,3-triazole ring exists in the crystal as the 2*H* isomer form. The UV–vis absorption spectra of these compounds correspond to the assembled spectra of ferrocene and aryl substitute groups, and the fluorescence spectra show a maximum at 374 nm in CH_2Cl_2. The cyclic voltammograms of **3b–3d** show the reversible oxidation waves of the ferrocenyl groups, and these waves anodically shift in comparison with ferrocene standard due to the electron withdrawing effect of the 1,2,3-triazoles ring. According to thermal polarizing microscopy and differential scanning calorimetry studies, compounds **3b–3d** display liquid crystal behaviors over wider mesophase range during first heating.

1. Introduction

Liquid crystalline compounds containing metallic atoms in their structure combine properties of the metal with those of the mesogens, leading to processable material with interesting magnetic, electronic, optical, and anisotropic properties. Ferrocene-containing liquid crystals represent a well-established family of metallomesogens [1]. Following the first report by Malthête and Billard in 1976 [2], sustained synthetic efforts led to an interesting variety of liquid crystalline ferrocenes, such as mono- [3–6], di- [7,8] and trisubstituted [9] ferrocenes, and ferrocenophanes [10,11]. These materials exhibit a rich mesomorphism.

On the other hand, liquid crystals containing heterocyclic units are of crucial importance in the design and synthesis of new advanced functional materials, where liquid crystalline phases, polarity, geometry, luminescence and other properties of the molecule may be varied through the introduction of high polar heteroatom [12,13]. The compounds containing five membered 1,2,3-triazole ring have attracted recent attention in the field of materials chemistry, organic chemistry, drug discovery, bioconjucations due to their high chemical stability, strong dipole moment (5.2–5.6 D) and aromatic character [14]. In the field of mesogenic materials, some liquid crystals containing 1,2,3-triazole ring have been synthesized, and exhibit multiform liquid-crystalline mesophases with a lower melting temperature and over a wide thermal range useful in device applications [15–17].

Ferrocene-based liquid-crystalline compounds containing heterocyclic rings such as pyrazole or oxadiazole unit in the rigid molecular core exhibited unique mesophases [18,19]. Though ferrocene-triazole conjugates have been applied in various fields such as conjugate chemistry, asymmetric catalysis, medicinal chemistry, host–guest interactions, and materials chemistry [20], however, to the best of our knowledge, there are no reports about ferrocene-triazole conjugates using in the liquid-crystalline materials to date. In this article, we synthesized a series of ferrocene derivatives containing 1,2,3-triazole ring. The designed molecular structures are shown in Scheme 1, where the naphthalene ring was supposed to lengthen of the rigid core and the chlorine atom was supposed to increase the molecule polarity. Thus, to balance the rigidity of molecules, terminal substituent was connected to the rigid core through an etheric bridge. Their liquid crystalline, redox and optical properties were studied.

---

* Corresponding author. Fax: +86 471 4992984.
E-mail address: bzx1957@sina.com (Z.-X. Bian).

http://dx.doi.org/10.1016/j.molstruc.2013.09.043

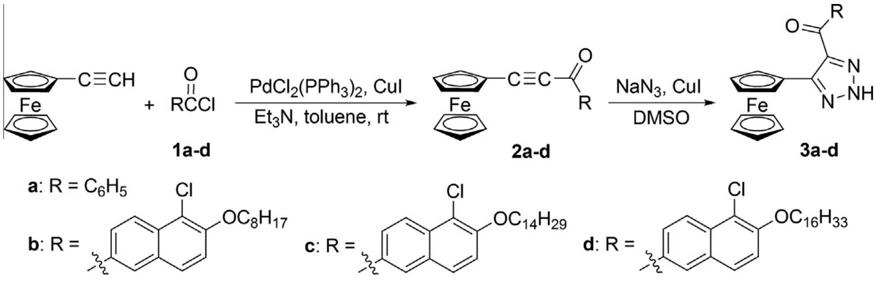

Scheme 1. Synthesis of compounds **2** and **3**.

2. Experimental

2.1. Materials

Ferrocenylethyne [21] and acyl chloride **1a–1d** [12] were prepared according to the reported procedures. Triethylamine and CH_2Cl_2 were distilled from calcium hydride before use. Toluene was dried and distilled from sodium. All other chemicals (AR) obtained from commercial sources were used without further purification.

2.2. Measurements

Fourier transform infrared spectroscopy (IR) spectra were recorded as KBr pellets on a NEXUS-670FT spectrometer. Nuclear magnetic resonance (NMR) spectra were recorded on an Avance 500 Bruker (500 MHz) spectrometer using tetramethylsilane as internal standard. The mass spectral analyses were obtained on the LCQ Advantage Max mass spectrometer (ESI source). Elemental analyses were carried out on a Perkin–Elmer-2400 apparatus. Electronic absorption spectra were recorded on analytikjena SPECORD.50 UV–vis spectrophotometer. Fluorescence spectra were obtained with VARIAN Cary Eclipse Fluorescence spectrophotometer. Differential scanning calorimetry (DSC) thermographs were obtained on a TA Q2000 at a heating rate of 10 °C min^{-1} under nitrogen flow. Thermooptical observations were carried out on a Leica DMLP polarizing optical microscope (POM) equipped with a THMS600 Linkam Heating and Freezing stage system at heating and cooling rate of 10 °C min^{-1} and Olympus BX51digital camera.

Cyclic voltammetry (CV) experiments were recorded on MEC-12B voltammetric analyzer and performed at room temperature in dry CH_2Cl_2 solutions containing 0.1 M tetra-*n*-butylammonium hexafluorophosphate ($TBAPF_6$) as a supporting electrolyte at a scan rate of 100 mV s^{-1}. A three-electrode configuration consisting of a glassy carbon working electrode, a Pt wire counter electrode, and an Ag/Ag^+ (in acetonitrile) couple reference electrode was used. The ferrocene/ferrocenium (Fc/Fc^+) couple was used as internal reference and showed a peak at +0.177 V vs $Ag/AgNO_3$. Prior to experiments, the system was purged with purified nitrogen gas to exclude dissolved oxygen from the solution.

2.3. General procedure for the synthesis of ferrocenyl ynones 2a–2d

A round-bottom sidearm flask (10 mL) containing $PdCl_2(PPh_3)_2$ (0.02 g, 0.03 mmol), CuI (0.0145 g, 0.075 mmol) and ferrocenylethyne (0.315 g, 1.5 mmol) was subjected to the Schlenk-line procedures of evacuation and purging of N_2 for three cycles. Acyl chloride **1** (2.25 mmol), Et_3N (0.32 mL, 2.25 mmol) and toluene (10 mL) were successively added, and the reaction mixture was stirred at room temperature until ferrocenylethyne disappeared by TLC test, then extracted with EtOAc. The combined organic phases were washed with brine, dried over anhydrous $MgSO_4$ and concentrated in vacuo. The residue was subjected to flash column chromatography with petroleum ether/EtOAc (10:1, V:V) as eluent, and the second fraction was the desired product which was recrystallized from petroleum ether/EtOAc (3:1, V:V) to afford the pure ynones **2**.

2.3.1. 3-Ferrocenyl-1-phenylprop-2-yn-1-one (2a)

Orange-red crystals, yield 78%, m.p. 120–122 °C; IR (KBr, ν_{max}) 3102, 2153, 1687, 1602, 1448, 1293, 1173, 1107, 1003, 823, 480 cm^{-1}; ^1H NMR (500 MHz, $CDCl_3$): δ 4.29 (s, 5H), 4.43 (s, 2H), 4.70 (s, 2H), 7.52 (dd, *J* = 7.2 Hz, 2H), 7.63 (d, *J* = 7.2 Hz, 1H), 8.20 (d, *J* = 7.2 Hz, 2H); ESI-MS *m/z*: calcd for M^+ 314.04, found: 314.08; Anal. calcd for $C_{19}H_{14}FeO$: C, 72.64; H, 4.49; Found: C, 72.80; H, 4.38.

2.3.2. 3-Ferrocenyl-1-(5-chloro-6-n-octoxynaphthalen-2-yl)prop-2-yn-1-one (2b)

Orange crystals, yield 53%, m.p. 100–102 °C; IR (KBr, ν_{max}): 3108, 2921, 2850, 2194, 1618, 1468, 1278, 1173, 1058, 1008, 823, 485 cm^{-1}; ^1H NMR(500 MHz, $CDCl_3$) δ 0.89 (t, *J* = 6.5 Hz, 3H), 1.30–1.39 (m, 8H), 1.53–1.56 (m, 2H), 1.89–1.92 (m, 2H), 4.22 (t, *J* = 6.4 Hz, 2H), 4.35 (s, 5H), 4.48 (s, 2H), 4.76 (s, 2H), 7.35 (d, *J* = 8.5 Hz, 1H), 7.93 (d, *J* = 8.5 Hz, 1H), 8.24–8.30 (m, 2H), 8.65 (s, 1H); ESI-MS *m/z*: calcd for M^+ 526.14, found: 526.19; Anal. calcd for $C_{31}H_{31}ClFeO_2$: C, 70.67; H, 5.93; Found: C, 70.45; H, 5.82.

2.3.3. 3-Ferrocenyl-1-(5-chloro-6-n-tetradecoxynaphthalen-2-yl)prop-2-yn-1-one (2c)

Orange crystals, yield 63%, m.p. 94–96 °C; IR (KBr, ν_{max}): 3093, 2921, 2852, 2149, 1619, 1462, 1260, 1100, 1027, 812, 474 cm^{-1}; ^1H NMR (500 MHz, $CDCl_3$) δ 0.89 (t, *J* = 6.5 Hz, 3H), 1.25–1.29 (m, 18H), 1.39–1.41 (m, 2H), 1.53–1.57 (m, 2H), 1.89–1.92 (m, 2H), 4.22 (t, *J* = 6.4 Hz, 2H), 4.31 (s, 5H), 4.45 (t, *J* = 1.7, 2H), 4.73 (t, *J* = 1.7, 2H), 7.36 (d, *J* = 9.0, 1H), 7.93 (d, *J* = 9.0 Hz, 1H), 8.25–8.31 (m, 2H), 8.66 (s, 1H); ESI-MS *m/z*: calcd for M^+ 610.23, found: 610.32; Anal. calcd for $C_{37}H_{43}ClFeO_2$: C, 72.73; H, 7.09; Found: C, 72.90; H, 7.01.

2.3.4. 3-Ferrocenyl-1-(5-chloro-6-n-hexadecoxynaphthalen-2-yl)prop-2-yn-1-one (2d)

Orange crystals, yield 73%, m.p. 92–98 °C; IR (KBr, ν_{max}): 3100, 2919, 2847, 2190, 1618, 1466, 1231, 1173, 1059, 1006, 825, 480 cm^{-1}; ^1H NMR (500 MHz, $CDCl_3$) δ 0.87 (t, *J* = 6.5 Hz, 3H), 1.24–1.28 (m, 22H), 1.39–1.41 (m, 2H) 1.53–1.56 (m, 2H), 1.89–1.92 (m, 2H), 4.23 (t, *J* = 6.5 Hz, 2H), 4.32 (s, 5H), 4.46 (t, *J* = 1.8 Hz, 2H), 4.74 (t, *J* = 1.8 Hz, 2H), 7.37 (d, *J* = 9.1 Hz, 1H)7.94 (d, *J* = 9.1 Hz, 1H), 8.23–8.31 (m, 2H), 8.67 (s, 1H); ESI-MS *m/z*: calcd for M^+ 638.26, found: 638.36; Anal. calcd for $C_{39}H_{47}ClFeO_2$: C, 73.29; H, 7.41; Found: C, 73.18; H, 7.52.

2.4. General procedure for the synthesis of ferrocenyl 1,2,3-triazoles 3a-3d

The ynones **2** (0.19 mmol), NaN_3 (0.19 g, 0.285 mmol), CuI (1.8 mg, 0.01 mmol) and DMSO (3 mL) were successively added to a round-bottom sidearm flask reacted at r.t. under N_2 until ynones disappeared by TLC test, then extracted with EtOAc. The combined organic phases were washed with brine, dried over anhydrous $MgSO_4$ and concentrated in vacuo. The residue was subjected to flash column chromatography with petroleum ether/EtOAc (5:1, V:V) as eluent, collecting the second fraction. The solvent was removed by a rotary evaporator to give the desired **3**.

2.4.1. Phenyl(5-ferrocenyl-2H-1,2,3-triazol-4-yl)methanone (3a)

Yellow crystals, yield 83%, m.p. 187 °C; IR (KBr, ν_{max}): 3151, 3093, 1659, 1600, 1555, 1445, 1293, 1173, 1107, 1003, 825, 509 cm^{-1}; ^1H NMR (500 MHz, D^6-DMSO) δ 4.06 (s, 5H), 4.49 (s, 2H), 5.10 (s, 2H), 7.56 (t, $J = 7.4$ Hz, 2H), 7.67 (t, $J = 7.4$ Hz, 1H), 8.05 (t, $J = 7.4$ Hz, 2H), 15.76 (s, 1H); ^{13}C NMR (125 MHz, D^6-DMSO) δ 179.59, 140.15, 137.80, 132.84, 129.99, 128.23, 69.47, 69.00; ESI-MS m/z: calcd for $[M+1]^+$ 358.06, found: 358.05; Anal. calcd for $C_{19}H_{15}FeN_3O$: C, 63.89; H, 4.23; N, 11.76; Found: C, 64.13; H, 4.17; N, 11.75.

2.4.2. (5-chloro-6-n-octoxynaphthalen-2-yl)(5-ferrocenyl-2H-1,2,3-triazol-4-yl)methanone (3b)

Purple-red crystals, yield 66%, m.p. 79.6 °C; IR (KBr, ν_{max}): 3143, 2921, 2851, 1615, 1469, 1279, 1163, 1058, 828, 504 cm^{-1}; ^1H NMR (500 MHz, $CDCl_3$) δ 0.88 (t, $J = 6.9$ Hz, 3H), 1.26–1.29 (m, 6H), 1.38–1.40 (m, 2H), 1.51–1.54 (m, 2H), 1.87–1.90 (m, 2H), 4.17–4.20 (m, 7H), 4.55 (s, 2H), 5.24 (s, 2H), 7.29 (d, $J = 8.5$ Hz, 1H), 7.84 (d, $J = 8.5$ Hz, 1H), 8.26–8.31 (m, 2H), 8.69 (s, 1H), 13.17 (s, 1H); ^{13}C NMR (125 MHz, $CDCl_3$) δ 186.63, 154.41, 134.27, 133.27, 130.04, 128.14, 126.98, 123.84, 117.28, 115.26, 71.29, 70.54, 69.97, 31.81, 29.70, 29.67, 29.31, 25.93, 22.67, 14.14; ESI-MS m/z: calcd for M^+ 569.15, found: 569.12; Anal. Calcd. for $C_{31}H_{32}ClFeN_3O_2$: C, 65.33; H, 5.66; N, 7.37; Found: C, 65.59; H, 5.93; N, 7.52.

2.4.3. (5-chloro-6-n-tetradecoxynaphthalen-2-yl)(5-ferrocenyl-2H-1,2,3-triazol-4-yl)methanone (3c)

Purple-red crystals, yield 66%, m.p. 74.1 °C; IR (KBr, ν_{max}): 3149, 2920, 2849, 1617, 1469, 1278, 1174, 1057, 825, 501 cm^{-1}; ^1H NMR (500 MHz, $CDCl_3$) δ 0.88 (d, $J = 6.8$ Hz, 3H), 1.38–1.26 (m, 20H), 1.50–1.55 (m, 2H), 1.85–1.91 (m, 2H), 4.09 (s, 5H), 4.18 (d, $J = 6.5$ Hz, 2H), 4.41 (s, 2H), 5.12 (s, 2H), 7.28 (d, $J = 9.0$ Hz, 1H), 7.83 (d, $J = 9.0$ Hz, 1H), 8.30 (s, 2H), 8.71 (s, 1H), 13.15 (s, 1H); ^{13}C NMR (125 MHz, $CDCl_3$) δ 186.58, 154.41, 154.28, 134.14, 133.15, 130.02, 129.89, 128.01, 126.89, 123.77, 117.14, 115.12, 77.28, 77.14, 77.02, 76.89, 69.84, 31.80, 29.57, 29.54, 29.47, 29.23, 29.19, 22.56, 14.00; ESI-MS m/z: 653.25 calcd for M^+, found: 653.23; Anal. calcd for $C_{37}H_{44}ClFeN_3O_2$: C, 67.94; H, 6.78; N, 6.42; Found: C, 68.21; H, 6.56; N, 6.35.

2.4.4. (5-chloro-6-n-hexadecoxynaphthalen-2-yl)(5-ferrocenyl-2H-1,2,3-triazol-4-yl)methanone (3d)

Purple-red crystals, yield 73%, m.p. 83.1 °C; IR (KBr, ν_{max}): 3152, 2919, 2850, 1633, 1614, 1468, 1278, 1168, 1059, 825, 503 cm^{-1}; ^1H NMR (500 MHz, $CDCl_3$) δ 0.88 (t, $J = 6.6$ Hz, 3H), 1.38–1.26 (m, 24H), 1.52–1.53 (m, 2H), 1.86–1.89 (m, 2H), 4.06 (s, 5H), 4.15 (t, $J = 6.5$ Hz, 2H), 4.37 (s, 2H), 5.11 (s, 2H), 7.26 (d, $J = 9.3$ Hz, 1H), 7.81 (d, $J = 9.3$ Hz, 1H), 8.29 (s, 2H), 8.71 (s, 1H), 13.90 (s, 1H); ^{13}C NMR (125 MHz, $CDCl_3$) δ 186.76, 154.40, 134.26, 133.30, 130.02, 128.12, 127.02, 123.84, 117.24, 115.22, 70.52, 70.11, 69.95, 69.55, 31.93, 29.71, 29.68, 29.67, 29.61, 29.58, 29.37, 22.70, 14.14; ESI-MS m/z: calcd for M^+ 681.28, found: 681.26; Anal. calcd for $C_{39}H_{48}ClFe\ N_3O_2$: C, 68.67; H, 7.09; N, 6.16; Found: C, 68.68; H, 6.83; N, 6.09.

Table 1
Crystal data and structure refinement for **3a**.

Compound	**3a**
Empirical formula	$C_{19}H_{15}FeN_3O$
Formula weight	357.19
T (K)	296(2)
Crystal system	Monoclinic
Space group	$P2_1$
a (Å)	8.6629(13)
b (Å)	9.3614(14)
c (Å)	9.8177(15)
α (°)	90
β (°)	96.521(3)
γ (°)	90
Volume (Å^3)	791.0(2)
Z, calc (mg m^{-3})	2, 1.500
Absorption coefficient (mm^{-1})	0.963
F(000)	368
Crystal size (mm^3)	$0.2 \times 0.2 \times 0.2$
θ range for data collection (°)	2.09–28.33
Reflections collected/unique	5686/3819 [$R_{(int)} = 0.0244$]
Observed reflections [$I > 2\sigma(I)$]	3262
Completeness to $\theta = 28.33$ (%)	99.50
Refinement method	Full-matrix least-squares on F^2
Data/restraints/parameters	3819/1/221
Goodness-of-fit on F^2	1.01
Final R indices [$I > 2$sigma (I)]	$R_1 = 0.0390$, $wR_2 = 0.0923$
R indices (all data)	$R_1 = 0.0487$, $wR_2 = 0.0976$

2.5. X-ray crystallography

Yellow single crystal of **3a**, suitable for X-ray diffraction analysis, was grown by slow diffusion of petroleum ether into a solution of **3a** in CH_2Cl_2 for about 2 weeks. Data were collected on a Bruker Smart APEX II CCD area detector with a Mo Kα radiation ($\lambda = 0.71073$ Å) at 296 K in the $\varphi - \omega$ scan mode. The structure was determined by direct method (SHELXS-97) and successive Fourier synthesis and refined by using the SHELXL-97 program. The nonhydrogen atoms were refined anisotropically, whereas the hydrogen atoms were placed in calculated positions and refined isotropically. Crystal data and structure refinement parameters are listed in Table 1. Selected bond distances and angles are placed in Electronic Supplementary information.

3. Results and discussion

3.1. Synthesis and characterization

The carbonylative coupling reaction of acyl chloride with ferrocenylethyne using $PdCl_2(PPh_3)_2$ (2%)/CuI (5%) as catalyst and Et_3N as base provided aryl ferrocenylethynyl ketones **2** in toluene [22]. The ynones then underwent the Cu(I)-catalyzed 1,3-dipolar cycloaddition with NaN_3 in DMSO at room temperature to form ferrocenyl 1,2,3-(NH)-triazoles **3** in excellent yields (Scheme 1) [23]. The chemical compositions of the synthesized compounds are in good agreement with the data of elemental analyses. The strong bands at 1659 cm^{-1} for **3a** and about 1615 cm^{-1} for **3b–3d** in the IR spectra may be assigned to the ketone carbonyl. Metal-ring vibrations of the ferrocene moiety are displayed in the long-wave area, at 474–509 cm^{-1}. In the ^1H NMR spectra, the triazole NH proton as a singlet appears at δ15.76 ppm (D^6-DMSO) for **3a** and 13.15–13.90 ppm ($CDCl_3$) for **3b–3d**.

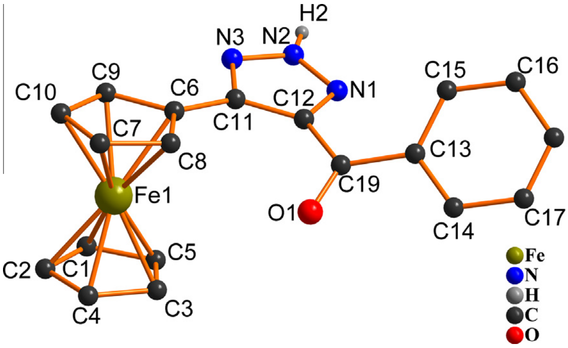

Fig. 1. X-ray structure of **3a**.

Table 2
UV–vis absorption and emission data of **3b–3d** in CH_2Cl_2.

Compound	Absorption λ_{max}, nm (log ε, L cm^{-1} mol^{-1})				Emission λ_{max}, nm
	I band	II band	III band	IV band	
3b	231 (4.70)	278 (4.60)	326 (4.21)	~480	374
3c	231 (4.71)	278 (4.61)	326 (4.20)	~480	374
3d	232 (4.69)	278 (4.59)	327 (4.20)	~480	374

The 1,2,3-(NH)-triazole **3a** was characterized by X-ray diffraction methods. The molecular structure of **3a** is shown in Fig. 1. The X-ray crystal structure reveals that **3a** exists in the crystal as the 2*H* (in the triazole ring) isomer form, however 1,2-di*H* tautomers equilibrium exists in neutral solution within these kinds of compounds [24]. The 1,2,3-triazole ring locates almost in the same plane of the substituted Cp ring, whereas staggered with benzene ring with the dihedral angle of 48.10(9)°. The distances of N(1)–N(2) (1.298(3)) and N(2)–N(3) (1.345(3)) are not equal. The distance of C(19)–O(1) double bond is 1.218(3) Å.

3.2. UV–vis absorption and fluorescence spectra

The photophysical properties of compounds **3b–3d** were investigated by UV–vis absorption and fluorescence spectra. The spectral data are summarized in Table 2. It can be seen that lengthening of the alkyl chain insignificantly changes the absorption and emission position of compounds **3b–3d**. The absorption and emission spectra of the representative compounds **3b** in CH_2Cl_2 at 3×10^{-5} M are shown in Fig. 2. As shown in Fig. 2, the UV–vis absorption spectra of **3b** correspond to assembled spectra of the ferrocene and the aryl substitute groups. The absorption bands below 280 nm are assignable to Fe(d)-π^* and π–π^* electronic transitions of the aromatic rings. The absorption band associated with the carbonyl chromophore shifted bathochromically to 330 nm due to the conjugational effect of the adjacent triazole ring and naphthyl group, overlapping with the B band of naphthalene ring. Very broad weak absorption bands at ~480 nm belong to d–d type transitions of the electrons of the iron atoms [25,26].

The maximum excitation wavelength of **3b** was 256 nm, and the emission spectrum taken at the maximum excitation wavelength in CH_2Cl_2 at 3×10^{-5} M was shown in Fig. 2 (insert). It can be found that the emission spectra with maximum emission 374 nm for compounds **3b–3d** are almost identical (Table 2).

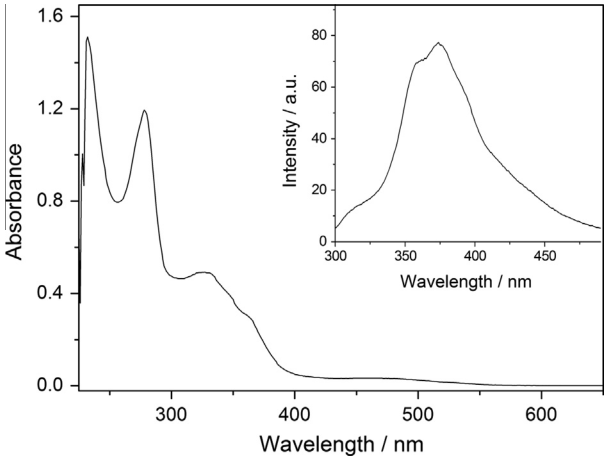

Fig. 2. UV–vis absorption and fluorescence spectra (insert) of **3b** in CH_2Cl_2.

Table 3
Electrochemical data for compounds **3b–3d** in CH_2Cl_2.

Compound	$E_{p,a}$[a]/V	$E_{p,c}$[b]/V	$E_{1/2}$[c]/V
Ferrocene	0.327	0.027	0.177
3b	0.304	0.214	0.259
3c	0.308	0.217	0.262
3d	0.312	0.219	0.266

[a] Anodic peak potential.
[b] Cathodic peak potential.
[c] $E_{1/2} = 1/2(E_{p,a} + E_{p,c})$.

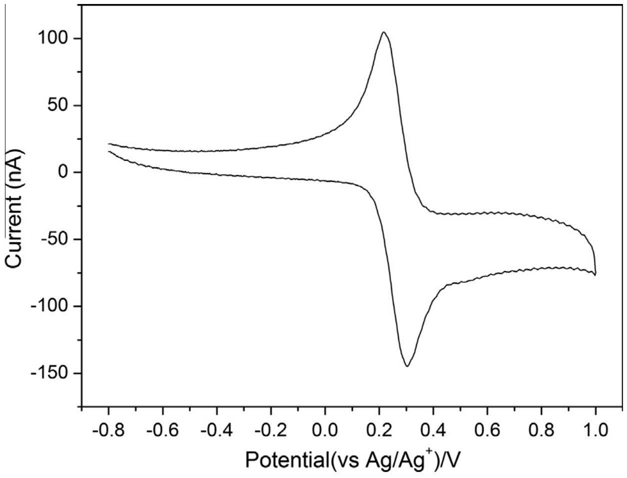

Fig. 3. CV curve of **3b** in CH_2Cl_2, 0.1 M $TBAPF_6$. Scan rate = 100 mV s^{-1}.

3.3. Electrochemical investigation

The electrochemical properties of compounds **3b–3d** were studied by CV using CH_2Cl_2 as the solvent containing 0.1 M $TBAPF_6$ as a supporting electrolyte. Electrochemical data are shown in Table 3. The CV curve of **3b** is shown in Fig. 3. As expected the redox-active ferrocenyl group exhibits a single reversible oxidation wave with formal redox potentials $E_{1/2}$ = 0.259, 0.262 and 0.266 V for **3b**, **3c** and **3d** respectively. As compared to the ferrocene standard ($E_{1/2}$ = 0.177 V), the potentials for **3b–3d** anodically shifted thereby suggesting an electron withdrawing effect of the 1,2,3-triazole ring on the ferrocene unit [27].

Table 4
Phase transition temperatures and associated enthalpies of compounds **3b–3d**.

Compound	Phase transitions[a] °C (ΔH/kJ mol^{-1})		
	First heating process	Second heating process	First cooling process
3b	C 79.6(11.9) M 143.7(22.3) I	28.5 T_g	30.5 T_g
3c	C 74.1(37.2) M 147.5(27.4) I	27.8 T_g 144.1 (0.4) I	28.3 T_g
3d	C 83.1 (39.7) M 143.1(22.9) I	27.2 T_g 140.0 (–) I	28.6 T_g

[a] C: crystal; M: mesophase; I: isotropic; T_g: glass transition.

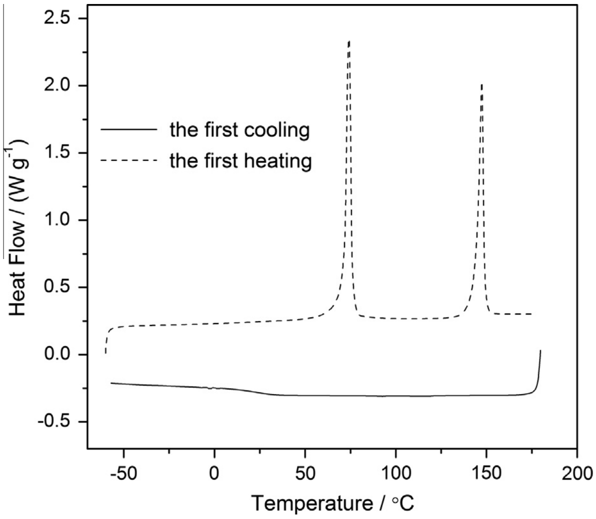

Fig. 4. DSC traces of **3c**.

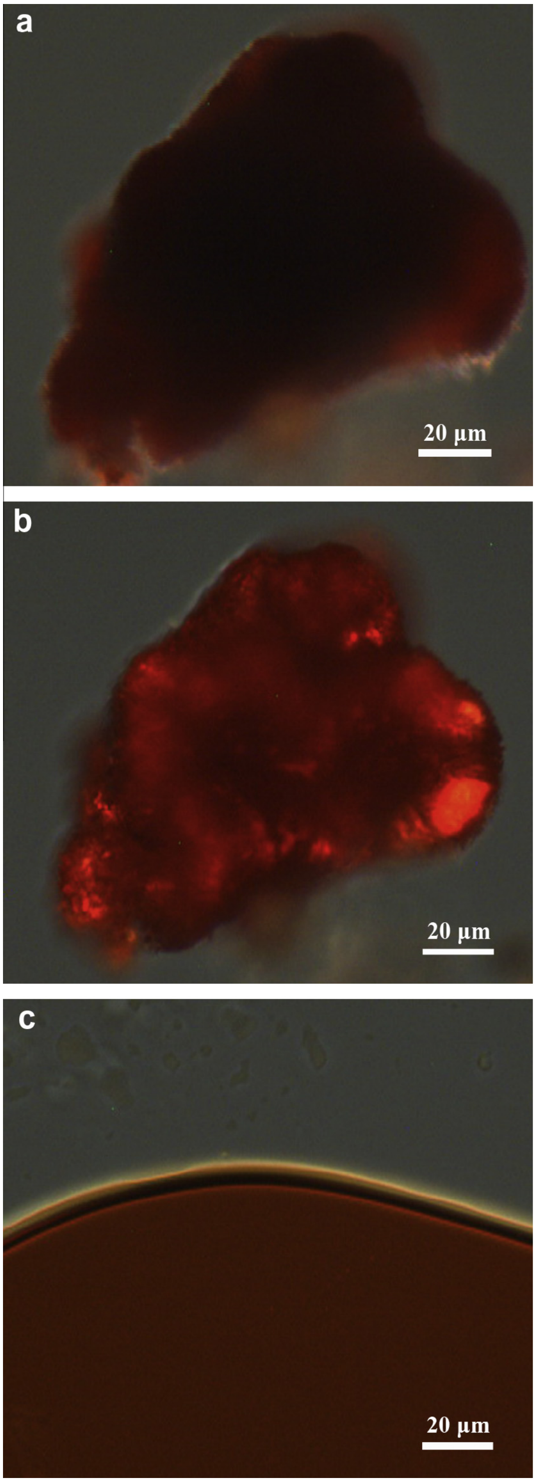

Fig. 5. POM images (20X) of **3c** at 25 °C (a), 140 °C (b) and 150 °C (c) on the first heating.

3.4. Mesomorphism

Liquid crystal properties of compounds **3b**–**3d** have been investigated by POM and DSC. The obtained data on the thermal behavior of the ligands **3b**–**3d** are presented in Table 4.

The ligands **3b**–**3d** all display liquid crystal behaviors. As an example, the DSC curves of **3c** are shown in Fig. 4. On the first heating, the compound exhibited an endothermic peak at which corresponds to the melting point at Tonset = 74.1 °C followed by the formation of a mesomorphic phase, and the second endothermic peak at Tonset = 147.5 °C, signifying the transition from the mesomorphic phase to the isotropic liquid, which was also confirmed by the POM images (Fig. 5). On first cooling from the isotropic liquid, a baseline shift was observed at 28.3 °C. The shape of the curve clearly resembles that of the typical glass transition point T_g of a DSC curve [16], which indicates the isotropic melt does not recrystallized but forms an isotropic glass in the cooling cycle. Similar thermal behaviors are observed in compounds **3b** and **3d**. On the second heating, the T_g was also observed in **3b**–**3d**. In addition, the weak endothermic peaks appeared at about 140–144 °C for compounds **3c** and **3d** during the second heating, but the enthalpies were very low (Table 4), which may be the formation of isotropic liquid.

Fig. 5 shows the typical POM images of the representative compound **3c**. From Fig. 5, we can see that compound **3c** shows the flower-like texture at 140 °C during first heating (Fig. 5b), and is in solid state and isotropic liquid state at 25 °C (Fig. 5a) and 150 °C (Fig. 5c), respectively. Whereas any textures are not found on cooling even below the T_g and the second heating, in agreement with the result of DSC experiment. As shown in Table 4, lengthening of the terminal alkyl chains from eight (**3b**) to fourteen (**3c**) carbon atoms gave rise to a wider mesophase range (73 °C) and lower melting point. Interestingly, a narrower mesophase range (60 °C) and high melting point (83.1 °C) were observed in **3d** when further lengthening terminal alkyl chains to sixteen carbon atoms.

4. Conclusion

A series of 1,2,3-(NH)-triazolylferrocene derivatives were synthesized and characterized. The crystal structure reveals that 1,2,3-triazole ring exists in the crystal as the 2*H* isomer form. These compounds exhibit good absorption, emission and electrochemical properties. The liquid crystal properties of these kinds of compounds were firstly investigated by thermal POM and DSC. The obtained metallomesogens are important footsteps toward the development of liquid crystal materials possessing polarizable heterocyclic rings, good redox activity and chemically stable ferrocene unit.

Acknowledgements

We thank the National Natural Science Foundation of China (NSFC, Nos. 21102068 and 21262023) and Natural Science Foundation of Inner Mongolia of China (No. 2013MS0207) for their generous financial support.

Appendix A. Supplementary material

CCDC 922173 contains the supplementary crystallographic data for compound **3a**. These data can be obtained free of charge via http://www.ccdc.cam.ac.uk/conts/retrieving.html, or from the Cambridge Crystallographic Data Centre, 12 Union Road, Cambridge CB2 1EZ, UK; fax: (+44) 1223-336-033; or e-mail: deposit@ccdc.cam.ac.uk.

Supplementary data associated with this article can be found, in the online version, at http://dx.doi.org/10.1016/j.molstruc.2013.09.043.

References

[1] J. Brettar, T. Bürgi, B. Donnio, D. Guillon, R. Klappert, T. Scharf, R. Deschenaux, Adv. Funct. Mater. 16 (2006) 260.
[2] J. Malthête, J. Billard, Mol. Cryst. Liq. Cryst. 34 (1976) 117.
[3] G. Lisa, D.A. Wilson, S. Curteanu, C. Lisa, C.-G. Piuleac, V. Bulacovschi, Thermochim. Acta 521 (2011) 26.
[4] K.C. Majumdar, S. Chakravorty, N. Pal, R.K. Sinha, Tetrahedron 65 (2009) 7998.
[5] O.N. Kadkin, E.H. Kim, S.Y. Kim, M.-G. Choi, Polyhedron 28 (2009) 1301.
[6] S. Campidelli, M. Séverac, D. Scanu, R. Deschenaux, E. Vázquez, D. Milic, M. Prato, M. Carano, M. Marcaccio, F. Paolucci, G.M.A. Rahman, D.M. Guldi, J. Mater. Chem. 18 (2008) 1504.
[7] N. Nakamura, S. Kagawa, Mol. Cryst. Liq. Cryst. 549 (2011) 150.
[8] W.A. Amer, L. Wang, H. Yu, A.M. Amin, Y. Wang, J. Inorg. Organomet. Polym. 22 (2012) 1229.
[9] P. Massiot, M. Impéror-Clerc, M. Veber, R. Deschenaux, Chem. Mater. 17 (2005) 1946.
[10] S.Y. Kim, O.N. Kadkin, E.H. Kim, M.-G. Choi, J. Organomet. Chem. 696 (2011) 2429.
[11] O.N. Kadkin, E.H. Kim, Y.J. Rha, S.Y. Kim, J. Tae, M.-G. Choi, Chem. -Eur. J. 15 (2009) 10343.
[12] H.C. Wang, Y.J. Wang, H.M. Hu, G.H. Lee, C.K. Lai, Tetrahedron 64 (2008) 4939.
[13] Y. Ren, W.H. Kan, M.A. Henderson, P.G. Bomben, C.P. Berlinguette, V. Thangadurai, T. Baumgartner, J. Am. Chem. Soc. 133 (2011) 17014.
[14] N. Gimeno, R. Martín-Rapún, S. Rodríguez-Conde, J.L. Serrano, C.L. Folcia, M.A. Pericás, M.B. Ros, J. Mater. Chem. 22 (2012) 16791.
[15] H. Gallardo, G. Conte, P.A. Tuzimoto, B. Behramand, F. Molin, J. Eccher, I.H. Bechtold, Liq. Cryst. 39 (2012) 1099.
[16] E. Beltrán, J.L. Serrano, T. Sierra, R. Giménez, J. Mater. Chem. 22 (2012) 7797.
[17] M.H. Ryu, J.W. Choi, H.J. Kim, N. Park, B.K. Cho, Angew. Chem. Int. Ed. 50 (2011) 5737.
[18] K.C. Majumdar, P.K. Shyam, Mol. Cryst. Liq. Cryst. 528 (2010) 3.
[19] K.C. Majumdar, P.K. Shyam, D.S.S. Rao, S.K. Prasad, Liq. Cryst. 39 (2012) 1117.
[20] V. Ganesh, V.S. Sudhir, T. Kundu, S. Chandrasekaran, Chem. Asian J. 6 (2011) 2670 (and references therein).
[21] M. Rosenblum, N. Brawn, J. Papenmeier, J. Organomet. Chem. 6 (1966) 173.
[22] Q.R. Lv, X. Meng, J.S. Wu, Y.J. Gao, C.L. Li, Q.Q. Zhu, B.H. Chen, Catal. Commun. 9 (2008) 2127.
[23] J. Li, D. Wang, Y. Zhang, J. Li, B. Chen, Org. Lett. 11 (2009) 3024.
[24] J.L.M. Abboud, C. Foces-Foces, R. Notario, R.E. Trifonov, A.P. Volovodenko, V.A. Ostrovskii, I. Alkorta, J. Elguero, Eur. J. Org. Chem. (2001) 3013.
[25] T. Mochida, H. Shimizu, S. Suzuki, T. Akasaka, J. Organomet. Chem. 691 (2006) 4882.
[26] W.Y. Liu, Y.S. Xie, B.X. Zhao, S. Lian, H.S. Lv, Z.L. Gong, D.S. Shin, Spectrochim. Acta A 76 (2010) 531.
[27] K.Q. Wu, J. Guo, J.F. Yan, L.L. Xie, F.B. Xu, S. Bai, P. Nockemann, Y.F. Yuan, Dalton Trans. 41 (2012) 11000.